*American Mineralogist, Volume 81, pages 550–560, 1996*

# In situ $^{29}$Si MAS NMR studies of structural phase transitions of tridymite

SIMON J. KITCHIN,[1] SIMON C. KOHN,[1,*] RAY DUPREE,[1,†]
C. MICHAEL B. HENDERSON,[2] AND KUNIAKI KIHARA[3]

[1]Department of Physics, University of Warwick, Coventry CV4 7AJ, U.K.
[2]Department of Earth Sciences, University of Manchester, Manchester M13 9PL, U.K.
[3]Department of Earth Sciences, Faculty of Sciences, Kanazawa University, Kanazawa 920, Japan

## ABSTRACT

The structural phase transitions of monoclinic tridymite that occur at elevated temperatures, as well as the structure of the high-temperature modifications, have been studied by $^{29}$Si MAS NMR. The sample, originating from the surface of a refractory silica brick, displays sharp discontinuities in the first moment ($M_1$), second moment ($M_2$), or both, of the $^{29}$Si MAS NMR spectrum at the following phase transitions: 108 ± 1 °C for the monoclinic (MC) to orthorhombic (OP) transition, 165 ± 5 °C for the transition from OP to a second orthorhombic phase (OS), and 206 ± 4 °C for the transition from OS to a third orthorhombic phase (OC). $M_1$ for the OC phase becomes more negative with increasing temperature up to ~323 °C, at which there is also a small discontinuity in $M_2$, indicating a transition from OC to a hexagonal phase (LHP). The spectrum of the MC phase consists of 12 narrow lines of equal area, consistent with the known crystal structure. The spectrum of the OP phase is broad and asymmetric, indicating a distribution of local environments at the Si sites. It can be simulated assuming an incommensurate structural modulation with a maximum amplitude of $\sim 5 \times 10^{-2}$ Å, but it is also consistent with a recent domain-formation model, provided that most disorder occurs at the Si6 site. The spectrum of the OS phase is asymmetric, indicating a nonlinear incommensurate modulation with a maximum amplitude of $\sim 2 \times 10^{-2}$ Å. The spectra of higher temperature phases are consistent with the single Si site of the known crystal structures, but $M_1$ values imply significantly smaller mean Si-O-Si angles $\langle\alpha\rangle$, e.g., $\langle\alpha\rangle$ = 152.6° at 220 °C from NMR, compared with 168.0° from X-ray diffraction data. This difference is consistent with disorder of O atoms around Si-Si axes.

## INTRODUCTION

The room-temperature structures of tridymite and the structural phase transitions that occur at elevated temperatures are extremely complex. At least three room-temperature polymorphs are known, each of which is subject to varying degrees of O disorder, stacking faults, etc. The number and nature of high-temperature structural modifications are even more complex, and the occurrence and temperature of phase transitions between them are affected by subtle differences in the room-temperature structure. In addition, the transition temperatures reported by different authors can vary by tens of degrees, and several different schemes of nomenclature exist, so it is not always simple to correlate the transition behavior of samples studied by different techniques.

Currently, the ordered monoclinic phase (MC) is probably the room-temperature polytype that is best understood. It contains 12 distinct Si sites, and the bond angles and distances are known (Baur 1977). At elevated temperatures (~110 °C) it becomes orthorhombic, and above approximately 400 °C it becomes hexagonal. Some workers (e.g., Nukui et al. 1978; Thompson and Wennemer 1979) have suggested that in synthetic samples three orthorhombic phases are involved: in order of increasing temperature, OP (orthorhombic with superlattice), OS an incommensurate structure, and OC, which contains just one Si site (nomenclature of Nukui et al. 1978). In meteoritic samples there appear to be two orthorhombic phases, OS and OC, unless the sample has been annealed in the stability field of the high-temperature hexagonal phase, in which case the OP phase also appears between MC and OS (Cellai et al. 1994). Until recently it was thought that there was just one hexagonal phase. However, De Dombal and Carpenter (1993) found evidence that the orthorhombic-to-hexagonal transition occurs in two stages with transitions at 350 and 465 °C. They also noted that observations made in previous studies indicate that these transitions occur in both natural and synthetic samples. In the high-temperature phases, OC and HP, X-ray diffraction studies have shown that there is considerable disorder in the O positions (Kihara et al. 1986a,

* Present address: Department of Geology, University of Bristol, Bristol BS8 1RJ, U.K.
† Author to whom all correspondence should be addressed.

0003–004X/96/0506–0550$02.00

1986b). The results of a recent electron diffraction study of Withers et al. (1994) suggest that this disorder is dynamic.

A factor that complicated many earlier powder X-ray diffraction studies is the partial transformation of crushed MC tridymite to another phase, known as MX1 (Hoffmann et al. 1983). The structure of this phase is less well known but is thought to be monoclinic and incommensurate (Hoffmann et al. 1983; Löns and Hoffmann 1987; Ashworth 1989; Xiao et al. 1995) and to undergo a transition to a phase of unknown structure at about 60 °C. Wennemer and Thompson (1984) and Graetsch and Flörke (1991) provided summaries of the earlier work on the various polymorphs of tridymite and their temperature dependencies, and these provide a good starting point for disentangling the complexities of tridymite structure types, phase-transition behavior, and nomenclature.

Recently, Xiao et al. (1993, 1995) published variable temperature MAS NMR spectra for MC tridymite grown from a $Na_2WO_4$ flux at 1400 °C. In the present study we show similar spectra and present a more detailed analysis of the behavior of an MC tridymite sample from the same source as that used in the X-ray diffraction studies of Kihara and coworkers (Kihara 1977, 1978; Kihara et al. 1986a, 1986b). This sample has a higher degree of order than those used by Xiao et al. (1993, 1995), thereby enabling additional information to be obtained.

## Samples and experimental details

The sample of tridymite used here was obtained from the surface of a refractory silica brick, which had been held at ~1200 °C for ~6 yr. It is known to be chemically pure (Kihara et al. 1986a), to be monoclinic at room temperature, and to show a series of sharp structural phase transitions. The crystal aggregates, which were <2 mm in diameter, were used without any further preparation. The individual crystals were <0.5 mm in diameter.

The $^{29}$Si MAS NMR experiments were performed on a Bruker MSL 360 spectrometer, operating at 71.54 MHz ($B_0 = 8.45T$), and using a Doty Scientific high-temperature MAS probe. Between 300 and 5000 transients were acquired for the spectra, with a $\pi/6$ pulse and a recycle delay of 11 s. Longer recycle delays (up to 30 s) were not found to change the relative intensities within the spectra. For the moment measurements fewer transients were acquired: between 328 and 164 for $T < 200$ °C and between 164 and 84 for $T > 200$ °C. The temperature was controlled by a home-built analog control unit, which was calibrated against the melting points of indium metal (156 °C) and cadmium metal (321 °C), as well as by performing a dummy heating experiment with a thermocouple inserted into the sample space. Additional heat-flux DSC experiments were performed using a Netzsch high-temperature DSC 404 system to provide independent measurements of the transition temperatures. For comparison with MC tridymite, DSC experiments were also performed on a sample of MX1 tridymite. This was obtained by crushing a portion of the MC tridymite sample by hand using an agate pestle and mortar. The $\alpha \leftrightarrow \beta$ transition of quartz was used for temperature calibration in the heat-flux DSC experiments.

## Results

### Heat-flux DSC

The DSC traces of MC tridymite showed two relatively narrow transitions, one at 108 °C (with a hysteresis of 23 °C) and one at 162 °C (with a hysteresis of 8 °C). The DSC traces for a crushed MX1 tridymite sample were very different. Five transitions were observed with increasing temperature at 78, 113, 121, 155, and 167 °C. Because MC tridymite is only partially transformed into MX1 tridymite when crushed (Hoffmann et al. 1983; Löns and Hoffmann 1987; Ashworth 1989; Xiao et al. 1995), the transitions at 113 and 167 °C can be associated with the remaining MC tridymite, whereas the transitions at 78, 121, and 155 °C can be assigned to the MX1 phase. The transitions of the crushed MX1 sample were much less well defined with decreasing temperature, with only three transitions observed at 135, 97, and 52 °C. These DSC experiments were performed to complement a $^{29}$Si MAS NMR study of MX1 tridymite. The preliminary NMR results were similar to those reported in the comprehensive NMR study of MX1 by Xiao et al. (1995). Hereafter, this paper therefore concentrates solely on the phases and phase changes of MC tridymite.

### The $^{29}$Si MAS NMR spectra

The room-temperature $^{29}$Si MAS NMR spectrum of MC tridymite (Fig. 1a) shows excellent resolution, with nine lines partially resolved. This is significantly better than previously published spectra (Smith and Blackwell 1983; Xiao et al. 1993, 1995) and suggests that the degree of long-range order is higher in this sample of MC tridymite than in those previously studied by $^{29}$Si MAS NMR. On increasing the temperature to ~108 °C the changes in the spectrum are quite small. The most noticeable changes are the loss of resolution of two peaks at ~114 ppm and the improvement of the resolution of separate peaks between ~109 and ~110 ppm. With further increases in temperature the spectrum changes abruptly into a broad asymmetric line >3 ppm in width (Fig. 1b). Above ~160 °C the spectrum changes dramatically, first to a far narrower, slightly asymmetric line (Fig. 1c) and then above ~210 °C to a narrow symmetrical line (Fig. 1d). Further increases in temperature to 450 °C produce only a small and gradual shift to low frequency (Fig. 1e).

The first and second moments of the spectra of MC tridymite were measured, with increasing temperature, between 21 and 450 °C. The $n$th moment is given by

$$M_n = \frac{\int_{-\infty}^{\infty} (\omega - \omega_0)^n f(\omega)\, d\omega}{\int_{-\infty}^{\infty} f(\omega)\, d\omega}. \quad (1)$$

The first moment ($M_1$) is a measure of the shift of the

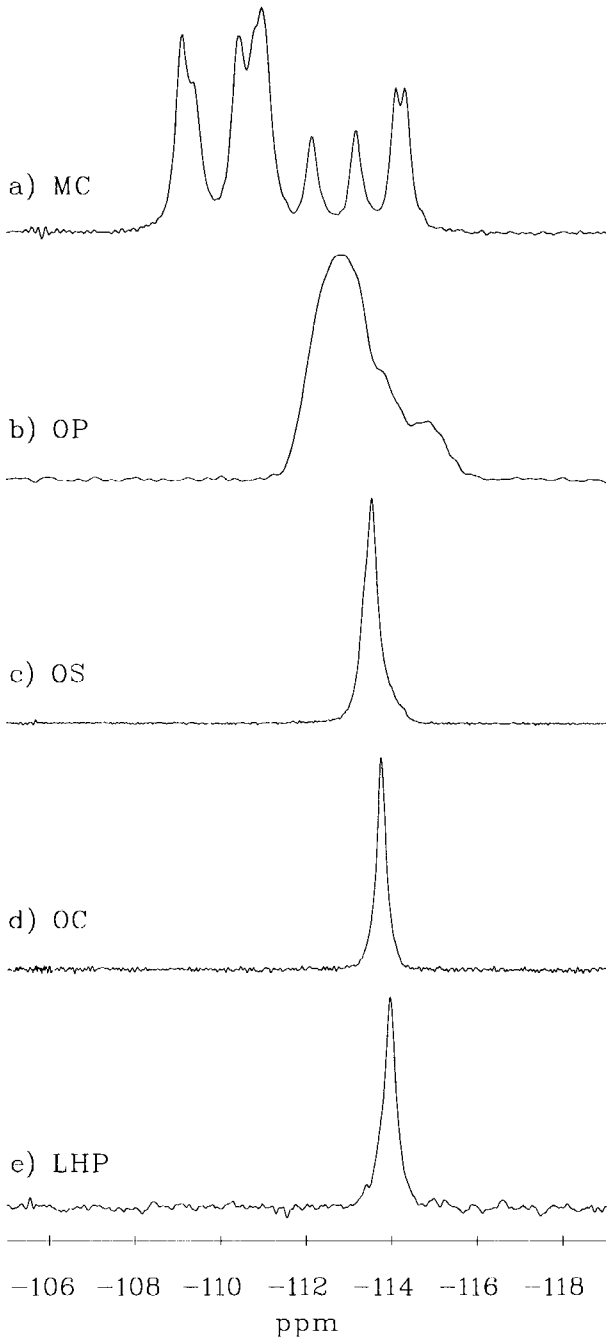


FIGURE 1. The $^{29}$Si MAS NMR spectra of tridymite at (a) 21, (b) 142, (c) 202, (d) 249, and (e) 401 °C. Spectrum e has 5 Hz of Lorentzian line broadening, whereas spectra a–d have no additional broadening.

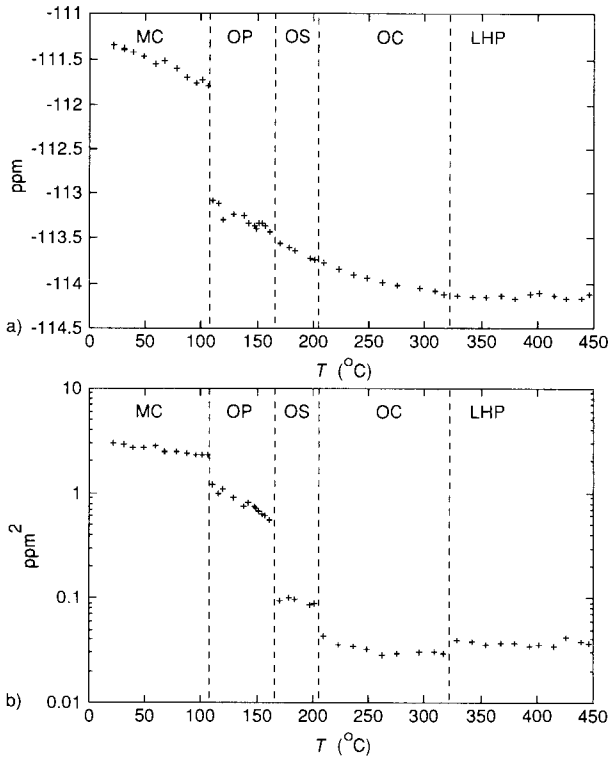


FIGURE 2. (a) First moment and (b) second moment of $^{29}$Si MAS NMR spectra of tridymite.

whole spectrum and in the case of a symmetrical line is identical to the mean shift. The second moment ($M_2$) is related to the width of the spectrum and is an indication of the magnetic inequivalence of different Si environments. However, calculations of $M_2$ using Equation 1 are severely affected by baseline artifacts and noise. To avoid these problems the intensity $f(\omega)$ was set to zero where $f(\omega)$ was less than or equal to three times the root-mean-square noise level. At temperatures above 200 °C the spectra were fitted to a pseudo-Voight function (Gaussian plus Lorentzian), and the second moment was then calculated from the fitted data.

$M_1$, plotted vs. increasing temperature in Figure 2a, was found to decrease from −111.3 ppm at 21 °C to −111.8 ppm at 106 °C. At 108 ± 1 °C there is a large discontinuity at which $M_1$ drops to ~113.1 ppm. With further increases in temperature $M_1$ steadily decreases to ~114.1 ppm at ~325 °C without further discontinuities and then remains virtually constant up to 446 °C, the highest temperature at which measurements were made. $M_2$, plotted vs. temperature in Figure 2b, decreases from ~3 ppm² at 21 °C to ~2.3 ppm² at 106 °C. At 108 ± 1 °C there is a discontinuity at which $M_2$ drops to ~1.2 ppm². Between 110 and 161 °C $M_2$ decreases rapidly to ~0.6 ppm². At 165 ± 5 °C there is another discontinuity at which $M_2$ drops to ~0.1 ppm². There is a further decrease to ~0.03 ppm² at 206 ± 4 °C and a small apparently discontinuous increase in $M_2$ to ~0.04 ppm² at 323 ± 6 °C. Although this last discontinuity is very small it is believed to be a significant effect because, although $M_2$ is approximately constant for $T > 323$ °C, all the measurements of $M_2$ for $T > 323$ °C are larger than those for $250 \leq T \leq 323$ °C.

## Discussion

### Transition temperatures

The discontinuities in the first and second moments (Fig. 2) and in the DSC experiments indicate the presence of four structural phase transitions in MC tridymite between room temperature and 450 °C. The phase transition marked at 108 ± 1 °C in the $M_1$ and $M_2$ measurements and in the DSC experiments can be assigned to a transition from MC to OP tridymite. The DSC traces did not show evidence that more than one transition is involved in the MC-to-OP transformation, in contrast to recent findings for meteoritic tridymite (Cellai et al. 1994). The transition temperature, 108 ± 1 °C, is close to that reported in X-ray diffraction studies of tridymite from the same source as this sample, $T_c \approx 105$ °C (Kihara 1977, 1978), and is in the middle of the range of transition temperatures ($100 \leq T \leq 115$ °C) that have been reported for both synthetic and naturally occurring tridymite (for examples, see Kihara 1977; Graetsch and Flörke 1991; Xiao et al. 1993; Dollase 1967; Cellai et al. 1994).

The two discontinuities in $M_2$ at 165 ± 5 °C and 206 ± 4 °C indicate that three orthorhombic phases are formed in this sample of tridymite at elevated temperatures. The transition at 165 ± 5 °C can be assigned to a transition from OP to OS tridymite, and the transition at 206 ± 4 °C can be assigned to a transition from OS to OC tridymite. In previous X-ray diffraction studies of samples from the same source as that studied here, only two orthorhombic phases were found: OP and OC (Kihara 1977, 1978). The OP → OS transition temperature is about 10 °C higher than that usually reported for other tridymite samples (Nukui et al. 1978; Graetsch and Flörke 1991; Xiao et al. 1993). The OS → OC transition temperature (206 ± 4 °C) is similar to that reported in a previous $^{29}$Si MAS NMR study of synthetic tridymite (Xiao et al. 1993) and some X-ray studies of synthetic tridymite (Graetsch and Flörke 1991). The transition is evident both in the $M_2$ data (Fig. 2) and as a disappearance of the low-frequency shoulder in the spectrum. It is significantly clearer in the $M_2$ data presented here than in those of Xiao et al. (1993). There is no detectable change, however, in $M_1$ and no heat-capacity anomaly in the DSC data. This behavior differs from that reported by Thompson and Wennemer (1979), in which there was a heat-capacity anomaly at the OS → OC transition. A wide range of OS → OC transition temperatures ($180 \leq T_c \leq 250$ °C) have been reported in other studies (Nukui et al. 1978; Cellai et al. 1994).

The small discontinuity in $M_2$ at 323 ± 6 °C is probably the result of an orthorhombic (OC) to hexagonal (LHP) transition. The transition temperature is lower than that recently reported for meteoritic tridymite (350 °C) by Cellai et al. (1994), and the discontinuity of ~0.01 ppm² is far smaller than the increase of ~0.4 ppm², at $350 \leq T_c \leq 400$ °C, reported by Xiao et al. (1993). The OC → LHP transition is also marked by a levelling off of the decrease in $M_1$ near 325 °C. A second-order transition from LHP to another hexagonal phase (HP), which was found at 420 °C in X-ray diffraction studies of a sample from the same source as that studied here (Kihara 1978), is not visible in either $M_1$ or $M_2$.

This series of phase transitions and the transition temperatures are very similar to those reported in the $^{29}$Si MAS NMR study of Xiao et al. (1993). The concentration of impurities, however, in the sample studied here is much lower than that in the sample studied by Xiao et al. (1993), which was grown from a $Na_2WO_4$ flux doped with 0.1 wt% $Fe_2O_3$. The only impurities that have been reported for samples from the same source as studied here are 50 ppm of Al and 140 ppm of Na (Kihara et al. 1986b). The concentration of impurities (Al, Na, Fe, etc.) is therefore probably not responsible for the different transition temperatures reported for tridymite samples from different sources.

### MC tridymite

The crystal structure of MC tridymite (Dollase and Baur 1976; Baur 1977) contains 12 inequivalent Si sites. The spectra, at temperatures below ~110 °C, were therefore fitted to 12 pseudo-Voight lines (Gaussian plus Lorentzian) of equal area. The Gaussian to Lorentzian ratio was adjusted until an appropriate value, 0.3, was found, and subsequently the ratio was fixed. The best fits were found to be in excellent agreement with the experimental data, strongly suggesting that the crystal structure of this sample and that of the meteoritic sample of Dollase and Baur (1976) are the same. The room-temperature spectrum and its best fit are shown in Figure 3, and the best-fit parameters are collected in Table 1. The successful fitting of 12 lines in a polymorph of $SiO_2$ of known structure provides an ideal opportunity to examine correlations of the shifts of the 12 lines with structural parameters determined from the X-ray diffraction studies (Baur 1977). [For a recent discussion of shift-structure correlations see Dupree et al. (1993).] Two correlations are shown in Figure 4: one a correlation of shift, $\delta$ (in parts per million), with the mean Si-Si distance, $\langle d \rangle$ (in angstroms), and the other a correlation of the shift, $\delta$ (ppm), with $\langle \cos \alpha/(\cos \alpha - 1) \rangle$, where $\alpha$ is an Si-O-Si angle (in degrees) and the angle brackets denote an average over the four values of $d$ or $\cos \alpha/(\cos \alpha - 1)$ at each Si site. The correlation equations are given by

$$\delta = -145.10\langle d \rangle + 335.51, \text{ esd} = 0.174 \quad (2)$$

for the mean Si-Si distance and by

$$\delta = -294.42\left\langle \frac{\cos \alpha}{\cos \alpha - 1} \right\rangle + 24.602, \text{ esd} = 0.222 \quad (3)$$

for the bond angle. It should be noted that while both of these correlations are very satisfactory, it has been assumed that the order of the lines (Table 1) is the same as the order of $\langle d \rangle$ or $\langle \cos \alpha/(\cos \alpha - 1) \rangle$ for each Si site. This may not be the case, particularly for sites with very similar shifts.

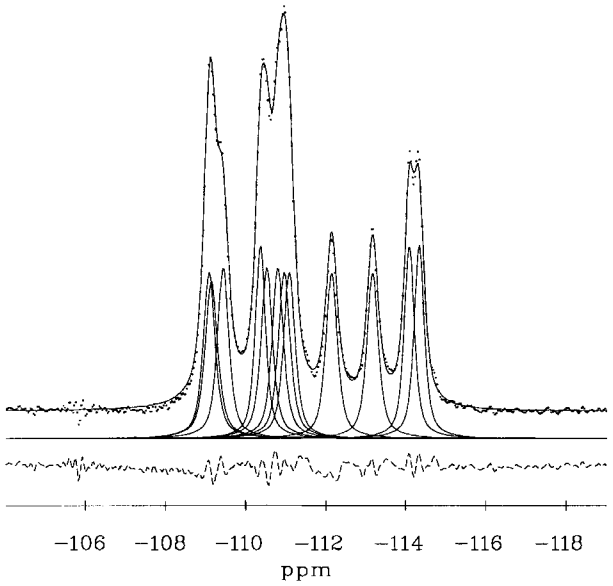


**FIGURE 3.** Room-temperature $^{29}$Si MAS NMR spectrum of monoclinic tridymite (dotted line, top) compared with simulation (solid line, top) using the parameters given in Table 1. The 12 peaks (solid lines, middle) were all constrained to have the same area, in accordance with the crystal structure of Dollase and Baur (1976). The dashed line (bottom) is the difference between the simulation and the spectrum.

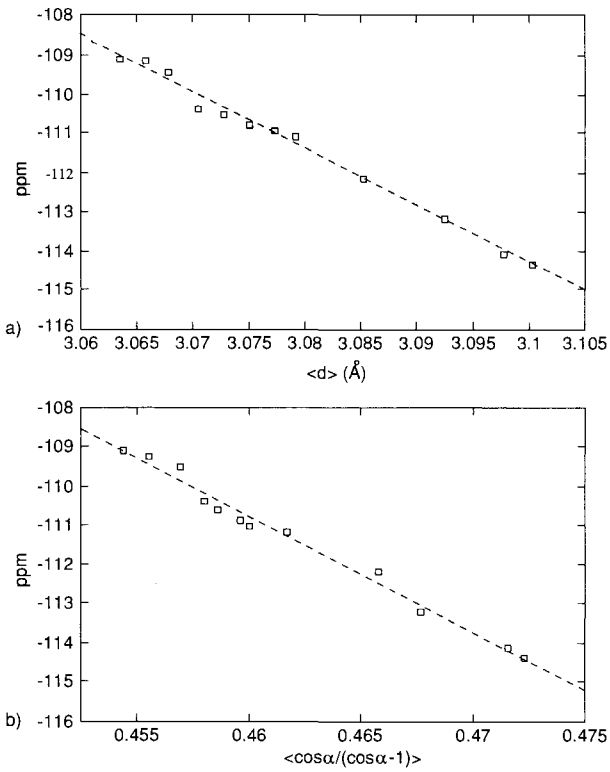


**FIGURE 4.** Correlations of $^{29}$Si chemical shift $\delta$ for MC tridymite at 21 °C with **(a)** mean Si-Si distance $\langle d \rangle$ for each Si site and **(b)** $\langle \cos \alpha/(\cos \alpha - 1) \rangle$, where $\alpha$ is an Si-O-Si angle and the angle brackets denote the mean for each site.

The applicability of these correlations can be assessed by including other silica polymorphs such as coesite, cristobalite, and quartz. For the distance correlation (Eq. 2) the inclusion of these polymorphs changes estimates of average Si-Si distances of <0.002 Å within the range $-109 \leq \delta \leq -114.5$ ppm. For the angle correlation coesite can be excluded because a mean value of $\langle \cos \alpha/(\cos \alpha - 1) \rangle$ is inappropriate (Engelhardt and Radeglia 1984; Pettifer et al. 1988) because of the very large range of Si-O-Si angles (~43°) at Si1. If quartz and cristobalite are added to the angle correlation (Eq. 3) changes in the estimated mean bond angle are <0.4° within $-109 \leq \delta \leq -114.5$ ppm. These small variations in the predicted mean angles and distances suggest that Equations 2 and 3 can be used to determine reliable values of $\langle d \rangle$ and $\langle \alpha \rangle$ at elevated temperatures, particularly for the higher temperature phases for which variations in the predictions are <0.3° for $\langle \alpha \rangle$ and <0.001 Å for $\langle d \rangle$ in the shift range of these phases ($-113 < \delta < -114.5$ ppm).

The coefficients in both Equations 2 and 3 are slightly different from those of previously published correlations. This is because earlier studies either used a smaller data set with less precise values of chemical shifts than those used here (Smith and Blackwell 1983) or included data from systems other than silica polymorphs (Engelhardt and Radeglia 1984). The most recent correlations, presented by Fyfe et al. (1993), were based on data from siliceous zeolites. Such correlations could well differ from those for silica polymorphs because the small contribution to the shifts from outer coordination spheres is affected by the voids in zeolite frameworks. Nevertheless,

**TABLE 1.** Simulated parameters (positions and widths) of MC tridymite at room temperature (21 °C)

| Line | 1 | 2 | 3 | 4 | 5 | 6 |
|---|---|---|---|---|---|---|
| Shift (ppm) | −109.08 | −109.14 | −109.43 | −110.36 | −110.52 | −110.80 |
| Width (ppm) | 0.35 | 0.37 | 0.34 | 0.30 | 0.34 | 0.34 |
| Line | 7 | 8 | 9 | 10 | 11 | 12 |
| Shift (ppm) | −110.96 | −111.09 | −112.14 | −113.16 | −114.08 | −114.33 |
| Width (ppm) | 0.35 | 0.34 | 0.34 | 0.34 | 0.30 | 0.30 |

*Note:* Numbering of lines is from high to low frequency in the spectrum in Figure 3. The width is the full-width at half-maximum intensity.

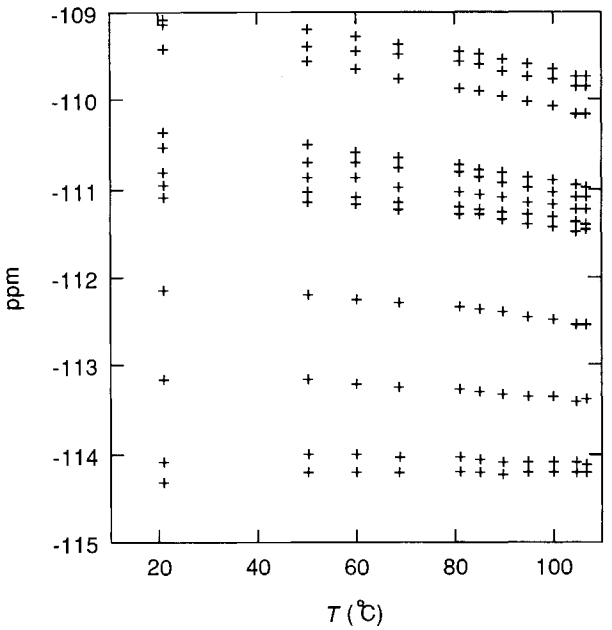


FIGURE 5. Shifts of the 12 lines fitted to spectra of tridymite in MC phase as a function of temperature.

in the region of interest for the higher temperature tridymite phases ($-113 < \delta < -114.5$ ppm) values of $\langle d \rangle$ and $\langle \alpha \rangle$ predicted using Fyfe et al.'s (1993) composite fit for ZSM-5 differ from those calculated using Equations 2 and 3 by <0.002 Å for $\langle d \rangle$ and <0.4° for $\langle \alpha \rangle$.

The effect of increasing temperature on the shifts of the 12 lines of the spectrum of MC tridymite is shown in Figure 5. The changes in the spectrum up to ~110 °C are small, with the peak positions moving by no more than −0.7 ppm, indicating that $\langle d \rangle$ increases by ≤0.005 Å and $\langle \alpha \rangle$ by ≤1.40°. The peaks with the least negative shifts (corresponding to Si sites with smaller mean Si-O-Si angles, $\langle \alpha \rangle$) move the most, whereas the peaks with the most negative shifts (and thus the largest values of $\langle \alpha \rangle$) remain virtually unchanged. There is almost no convergence of the lines at or below the transition temperature, indicating that the MC → OP transition is first order. This contrasts with some structural phase transitions in other framework silicates such as the tricritical $P\bar{1} \rightarrow I\bar{1}$ transition in anorthite (Phillips and Kirkpatrick 1995).

## OP tridymite

The unit cell of OP tridymite is closely related to that of OC tridymite with an additional superstructure of threefold period along the *a* direction (Kihara 1977) resulting in a structure containing six inequivalent Si positions. The $^{29}$Si MAS NMR spectra in Figure 6 show virtually no resolution of lines from the individual sites throughout the temperature range for this phase ($108 \leq T \leq 165$ °C). The magnitude of the displacement parameters (Kihara 1977) suggests that this broadening of the spectrum may be the result of static disorder. The vibrational ellipsoids of the O atoms suggest that they are disordered about the Si-Si axes (Kihara 1977), whereas the magnitude of the vibrational ellipsoids of the Si atoms is ~3 times greater in the OP phase than in the MC phase

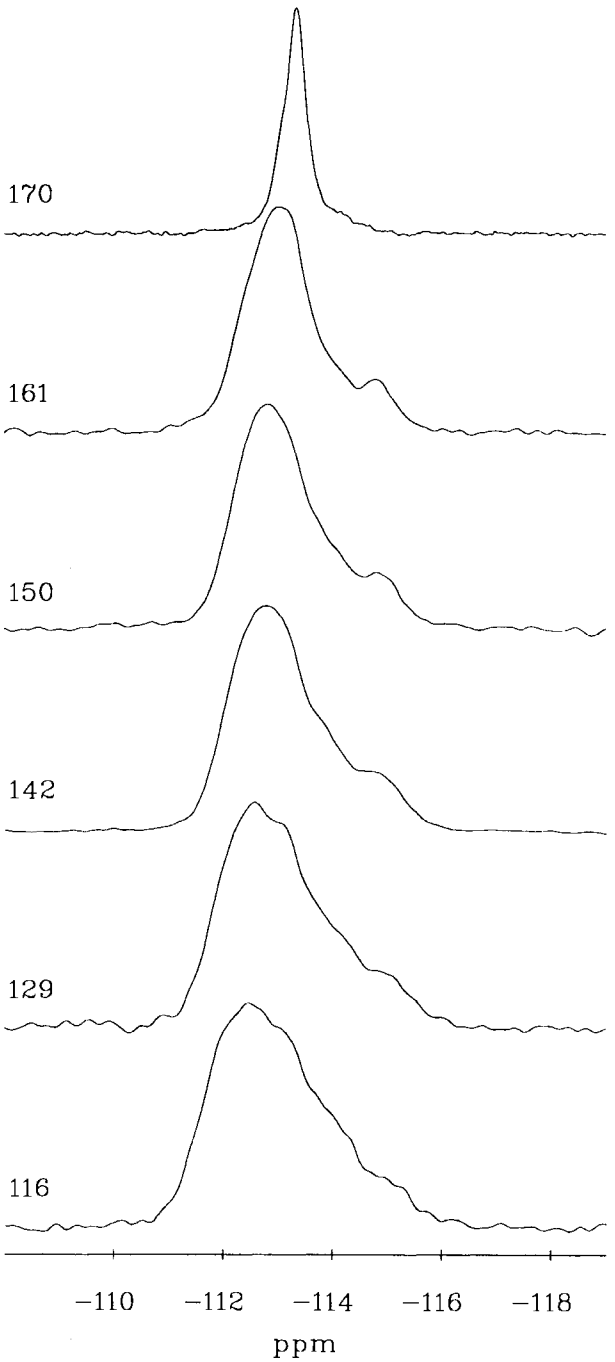


FIGURE 6. The $^{29}$Si MAS NMR spectra of OP tridymite at several temperatures and OS tridymite at 170 °C. The temperatures (in degrees Celsius) are given to the left of each spectrum. Ten Hz of Lorentzian line broadening was applied to each spectrum.

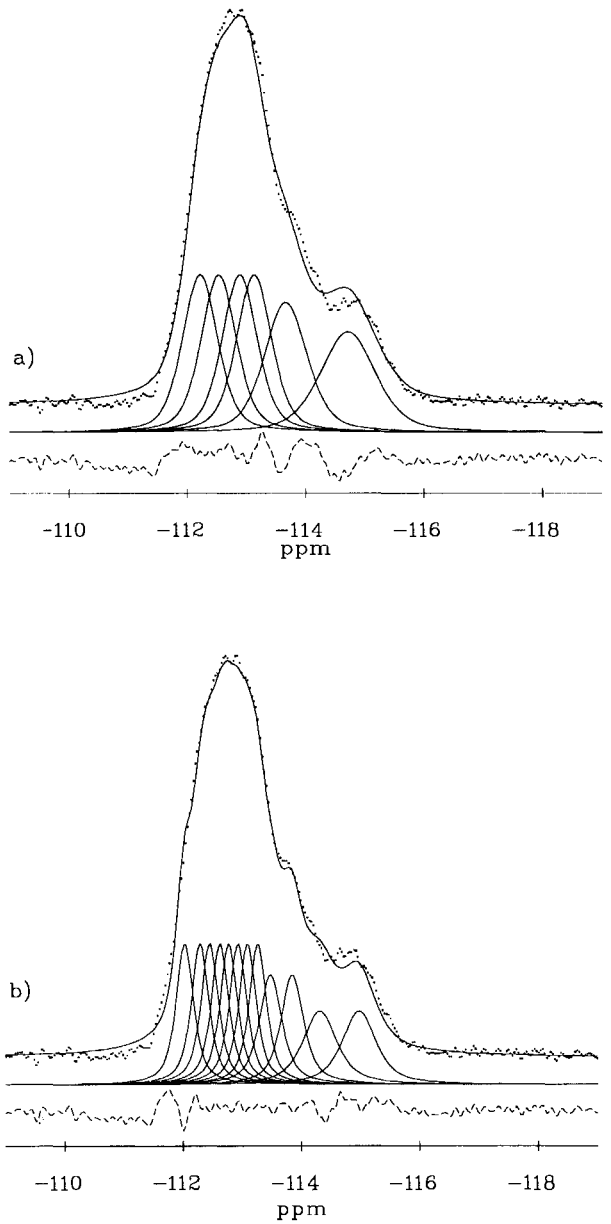


FIGURE 7. The $^{29}$Si MAS spectrum of OP tridymite at 142 °C compared with simulations using (a) six pseudo-Voight lines and (b) 12 pseudo-Voight lines of equal area but unequal width. The dotted lines are the experimental points, the solid lines are the simulations, and the dashed lines are the difference between the spectrum and simulations.

(Baur 1977; Kihara 1977), suggesting that there may also be some disorder in the Si positions. Static disorder in the O positions alone, without disorder in the Si positions, would not be expected to broaden the spectrum significantly unless accompanied by variations in bond lengths, which are considered unlikely.

Initial simulations of the spectra consisted of six lines of equal area. To achieve a reasonable fit the width of the lines (full-width at half-maximum) had to vary and be far greater than the widths in the MC phase. The best fit of the spectrum at 142 °C (Fig. 7a) was achieved with a width of 0.7 ppm for lines corresponding to Si1 to Si4 [using the numbering of Kihara (1977)] and 0.85 and 1.1 ppm for lines corresponding, respectively, to Si5 and Si6. These lines are at least twice the width of those in the spectra of the MC phase and in the spectra of the higher temperature phases OC and LHP. This suggests that if there are no more than six Si sites in the structure then there is static disorder in all the Si sites, with Si5 and Si6 affected more than Si1 to Si4. Even with these larger line widths, however, accurate simulation of the relative intensities of the high- and low-frequency halves of the spectrum was found to be impossible. This is shown in Figure 7a in which the intensity of the simulation is satisfactory for $-112 \leq \delta \leq -114$ ppm but is too high for $-114 \leq \delta \leq -115$ ppm.

Very recently Kihara (1995) reanalyzed the structures of some of the high-temperature phases of tridymite in terms of domain-formation models, using a distance least-squares method (Kihara 1995). These calculations suggest that there are probably 12, but possibly as many as 36, symmetrically independent Si sites in OP tridymite (Kihara 1995). To test whether a 12-site structure is consistent with the $^{29}$Si MAS NMR spectrum, simulations were performed involving 12 lines of equal area, with widths no larger than the average line width in the MC phase. To achieve reasonable fits, however, the width of lines at the low-frequency side of the spectrum, corresponding to Si5 and Si6, had to be increased from 0.34 ppm to 0.45 and 0.67 ppm, respectively (Fig. 7b), as was found in the six-site simulations. Si5 and Si6 are adjacent to the domain boundaries in the model of Kihara (1995), and thus stresses arising from distortion of the structure at the domain boundaries may cause these sites to be more disordered. This disorder can be estimated, using Equation 2, to involve displacements of the Si sites by $\leq 2 \times 10^{-3}$ Å. Although these simulations could be extended to 36 sites this would not be a useful test of these models because of the large number of parameters involved.

An alternative explanation is that the broadening of the spectra of the OP phase is the result of an incommensurate structural modulation (Xiao et al. 1993). In such a situation, in which the modulation wavelength is incommensurate with the periodicity of the underlying structure, the displacement $U$ of an Si site from its position in a hypothetical undistorted structure can be written as $U = A \cos \phi(x)$ (Blinc 1981). If it is assumed that this modulation can be described by a plane wave of wavelength $\lambda$ with an initial phase $\phi_0$, then

$$\phi(x) = 2\pi \frac{x}{\lambda} + \phi_0. \quad (4)$$

The $^{29}$Si resonance frequency, which depends on the displacement $U$, thus varies continuously with the position $x$ of the Si site along the modulation wave leading to a

characteristic broadening of the NMR spectrum. The resonance frequency $\nu$ can be expressed as an expansion in powers of the displacement and thus to second order is given by

$$\nu = \nu_0 + \nu_1 A \cos \phi(x) + \tfrac{1}{2}\nu_2 A \cos^2 \phi(x). \quad (5)$$

To simulate spectra of the OP phase broadened by an incommensurate modulation, 500 evenly spaced values of $\phi$ were used, spanning one period of the modulation wave. Values of $\nu$ were calculated with the expansion (Eq. 5) restricted to first order, i.e., $\nu_2 = 0$. The resulting line shape, convoluted with a pseudo-Voight function, gave the spectrum for one Si site. Six such simulations, representing Si1 to Si6, were combined to fit the experimental spectrum.

Attempts to fit the spectrum using the same value of $\nu_1$ at each site were unsatisfactory. Simulations with larger values (e.g., $0.55 < \nu < 0.65$ ppm) fitted the low-frequency half of the spectrum ($-113.5 \leq \delta \leq -115$ ppm) well but the high-frequency half ($-112 \leq \delta \leq -113.5$ ppm) poorly, whereas for smaller values (e.g., $0.45 < \nu < 0.55$ ppm) this situation was reversed. Thus, it was necessary to use an amplitude $\nu_1$ varying from 0.11 ppm for Si1 to 0.28 and 0.54 ppm for Si5 and Si6, respectively. The best fit achieved in this way is shown in Figure 8.

The changes in the mean Si-Si distance $\Delta\langle d\rangle$ caused by the modulation were calculated from the fitted values of $\nu_1$ and Equation 2 to be between $\sim 1.4 \times 10^{-3}$ Å for Si1 and $\sim 7.4 \times 10^{-3}$ Å for Si6. The amplitude of the modulation was estimated using the largest value of $\Delta\langle d\rangle$, with $\lambda = 100$ Å, and the model of Xiao et al. (1995) to be $\sim 0.05$ Å.

The presence of an incommensurate modulation within the temperature range for the OP phase was reported by Dollase (1967). That work, however, studied meteoritic rather than synthetic tridymite, and recent evidence (Cellai et al. 1994, 1995) suggests that meteoritic MC tridymite transforms directly to the OS phase with no intermediate OP phase unless annealed in the stability field of the hexagonal phase.

The shift correlations determined for MC tridymite at 21 °C (section) and the first moment of the OP tridymite spectra can be used to determine the mean Si-Si angles, $\langle\alpha\rangle$, and Si-Si distances, $\langle d\rangle$, in the OP phase. The values of $\langle\alpha\rangle$ and $\langle d\rangle$ determined from the first moment at 154 °C are $\langle\alpha\rangle = 151.9°$ and $\langle d\rangle = 3.09$ Å. The value of $\langle d\rangle$ is in agreement with the single-crystal X-ray diffraction data collected at 155 °C (Kihara 1977) ($\langle d\rangle = 3.09$ Å). The value of $\langle\alpha\rangle$ determined from the X-ray data, however, is 5.4° larger than that determined from NMR if the X-ray data are uncorrected for disorder. This discrepancy, which was also noted by Xiao et al. (1993), results from the large prolate-spheroidal vibrational ellipsoids of the O atoms in the X-ray data (Kihara 1977). The Si-O-Si angles $\alpha$ determined by X-ray diffraction are thus averages over mean O positions, whereas the angles $\langle\alpha\rangle$ determined by NMR are averages over the true Si-O-Si bond angles for the Si sites.

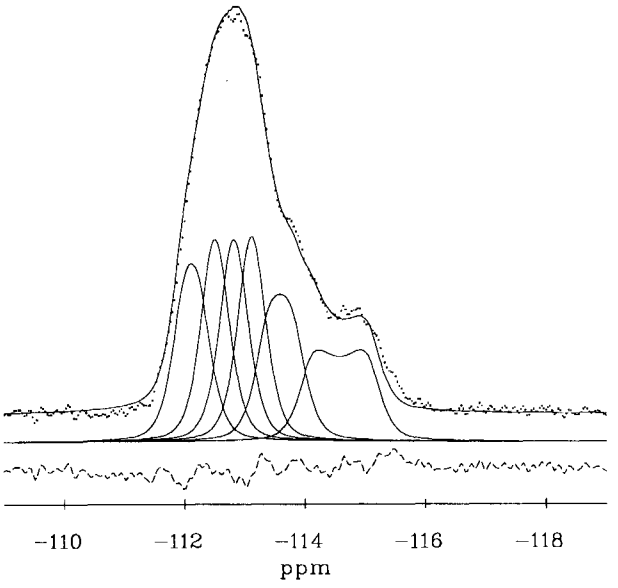


**FIGURE 8.** The $^{29}$Si MAS spectrum of OP tridymite at 142 °C (dotted line, top) compared with a simulation (solid line, top) of six lines (solid lines, middle) each broadened by an incommensurate plane-wave modulation. The modulation for each site (in order of lines from left to right) is as follows: Si4 $\nu_1 = -0.19$ ppm, Si2 and Si3 $\nu_1 = -0.12$ ppm, Si1 $\nu_1 = -0.11$ ppm, Si5 $\nu_1 = -0.28$ ppm, Si6 $\nu_1 = -0.54$ ppm, with $\nu_2 = 0$. The line shape for each site was convoluted with a pseudo-Voight function with full-width at half-maximum of 0.4 ppm.

## OS tridymite

The OS phase, unlike the OP phase, is generally thought to have a single Si site, with an incommensurate modulation along [100] (Nukui et al. 1978; Graetsch and Flörke 1991). The modulation wavelength decreases from 95 Å just above the OP → OS transition to 65 Å just below the OS → OC transition (Nukui et al. 1978; Graetsch and Flörke 1991). The amplitude of this modulation has been estimated to be ~0.3 Å from diffraction data (Nukui et al. 1979). A recent analysis of the width of the $^{29}$Si MAS NMR spectrum, however, suggests it is ~0.02 Å (Xiao et al. 1995).

The $^{29}$Si MAS spectrum of OS tridymite at 202 °C is shown in Figure 9. The asymmetry of the spectrum is probably the result of nonlinearity of the modulation, i.e., the modulation is not a plane wave. Asymmetry, however, can also arise in the plane-wave limit if higher order terms in the frequency expansion (Eq. 5) are nonzero. This is unlikely in the present case because the degree of asymmetry in the spectrum would require large third- or higher order terms in Equation 5.

To simulate the spectra an approximate solution to the sine-Gordon equation was used (Blinc 1981; Phillips et al. 1991):

$$\phi(x) = \sum_{l=0} \frac{4}{p} \arctan \exp[\alpha(x - l\beta)] + \phi_0 \quad (6)$$

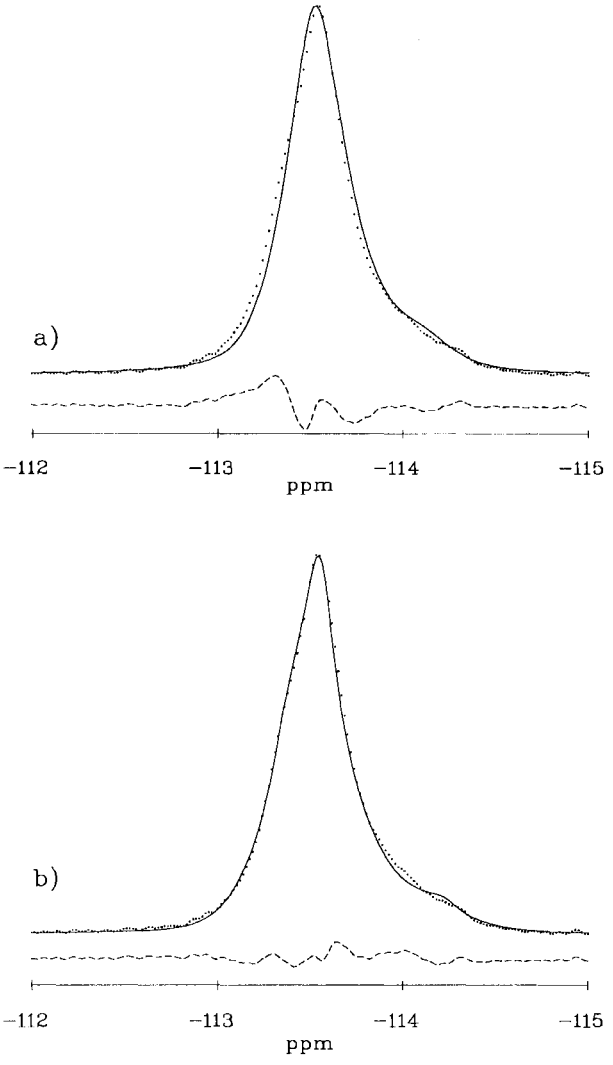


FIGURE 9. The $^{29}$Si MAS spectrum of OS tridymite at 202 °C compared with simulations of one site with a nonlinear incommensurate modulation. (**a**) Spectrum compared with simulation with $n_s = 0.17$, $p = 1$, $\phi_0 = 180°$, $\nu_1 = -0.32$ ppm, and $\nu_2 = 0$ ppm, and (**b**) compared with simulation with $n_s = 0.32$, $p = 1$, $\phi_0 = 180°$, $\nu_1 = -0.3$ ppm, and $\nu_2 = -1.0$ ppm. For both simulations the incommensurate line shape was convoluted with a pseudo-Voight function with full-width at half-maximum of 0.3 ppm.

where $\pi/\alpha$ is the soliton width, $\beta$ is the intersoliton spacing, and the soliton density ($n_s$) is given by $n_s = \pi/(\alpha\beta)$. In the context used here the solitons are phase-domain walls, regions in which the phase changes rapidly by $2\pi/p$. The solitons are separated by commensurate regions in which the phase is constant. The soliton density is thus a measure of the fraction of nuclei that are within the domain walls. The symbol $p$ is the ratio of the low-temperature unit-cell edge $a'$ to the high-temperature unit-cell edge $a$. In this case, however, even though $a$ for OP is three times that of the higher temperature phase (OC), $p = a'/a$ is not necessarily 3 because just above the OP → OC transition temperature $\lambda \neq a'$, i.e., the transition is not a lock-in transition.

Simulations of the OS spectra were obtained using the same methods described for the OP phase with the exception that Equation 6 was used to calculate $\phi$ for evenly spaced values of $x$ spanning one period of the modulation wave. A simulation using only first-order terms in the expansion, Equation 5, is shown in Figure 9a. Although the fit to the experimental spectrum is far from perfect, this simulation does reproduce the main features of the spectrum: a large peak arising from commensurate regions in the structure and a tail on the low-frequency side of the spectrum arising from the solitons or phase-domain walls. Several attempts were made to improve this simulation, in particular to reproduce the small shoulder on the high-frequency side of the commensurate peak using $p \geq 1$ and $\nu_2 > 0$. Small but significant improvements in the fit were achieved with $p = 1$ and $\nu_2 > 0$ (Fig. 9b).

The maximum change in the mean Si-Si distance ($\Delta\langle d\rangle$) caused by the modulation can be calculated from the fitted values of $\nu_n$ and Equation 2 to be $\sim 3.5 \times 10^{-3}$ Å. The actual amplitude of the modulation, determined using this value of $\Delta\langle d\rangle$ and the model of Xiao et al. (1995), is $\simeq 0.02$ Å.

Another possible cause of at least some of the asymmetry of the spectrum is that throughout the temperature range of the OS phase the sample is a mixture of OC and OS phases, some crystals having transformed directly from OP to OC. The OC crystals would give rise to the large commensurate peak, and OS crystals would cause the tail on the low-frequency side of the spectrum. Simulations of this model involving a pseudo-Voight line (OC) and a line shape of a plane-wave, incommensurately modulated phase (OS) were unable to reproduce the shoulder on the high-frequency side of the spectrum. Similar simulations involving a nonlinear modulation with $n_s > 0.32$ successfully fitted the spectrum, even if $\nu_2 = 0$. Because the spectra of OS presented here, however, are very similar those of Xiao et al. (1993, 1995), OC and OS phases would have to be present in very similar proportions for two samples of very different origin. We therefore consider this possibility to be unlikely.

### OC and hexagonal tridymite

The spectrum of the OC phase (Fig. 1d) is a single narrow line that is symmetrical, which is consistent with the single Si site of the published crystal structure (Dollase 1967; Nukui et al. 1978; Kihara et al. 1986b). Recently, however, Kihara suggested that there may be two inequivalent Si sites in the structure (Kihara 1995). The width of the $^{29}$Si spectrum is no larger than the average line width in the MC phase, which indicates that if the two Si sites are present they are dynamically averaged at frequencies greater than ~0.1 kHz. The line width is therefore unaffected. This is in contrast to the lower tem-

perature OP phase, the spectrum of which is broadened by static disorder.

The second moment of the spectra of the OC phase (Fig. 2b), varying between 0.044 ppm$^2$ at 210 °C and 0.029 ppm$^2$ at 317 °C, is significantly smaller than the value of ~0.1 ppm$^2$ reported by Xiao et al. (1993). This difference can be attributed to a higher degree of long-range order in the sample. The first moment (Fig. 2a), varying from −113.77 ppm at 210 °C to −114.11 ppm at 317 °C, is slightly less negative than the value reported by Xiao et al. (1993) (~ −114.4 ppm), suggesting that the mean Si-O-Si angle $\langle\alpha\rangle$ is slightly smaller in the sample studied here. Using the correlation given by Equation 3 $\langle\alpha\rangle$ increases from 152.6° at 210 °C to 153.1° at 317 °C. This compares with values of 170.1° (Dollase 1967) and 168.0° (Kihara et al. 1986b) determined by single-crystal X-ray diffraction at 220 °C. As in lower temperature orthorhombic phases the mean Si-O-Si angles determined by NMR are means of the actual angles. The larger X-ray values result from O disorder (Kihara et al. 1986a, 1986b). The Si-Si distances, however, are almost in agreement: $\langle d\rangle$ = 3.09 Å from X-ray diffraction (Dollase 1967) and $\langle d\rangle$ = 3.10 Å from NMR (using Eq. 2).

The spectrum of the LHP phase (Fig. 1e), like that of the OC phase, consists of a single narrow line that is symmetrical, in agreement with the single Si site of the published crystal structure (Kihara et al. 1986b). The first moment of the NMR spectrum is the same in the LHP phase as in the OC phase at 317 °C. The mean Si-O-Si angle $\langle\alpha\rangle$ and Si-Si distance $\langle d\rangle$ in LHP tridymite are the same as they are in OC tridymite (~153°, 3.10 Å). The mean bond angle from X-ray diffraction, if uncorrected for disorder, is larger, $\langle\alpha\rangle$ = 172.6° (Kihara et al. 1986b). This is because the oblate-spheroidal vibrational ellipsoids of the O atoms are larger in the X-ray structure of LHP than they are in OC, i.e., the O disorder is greater in LHP (Kihara et al. 1986b).

At 420 °C X-ray diffraction studies showed a phase change to another hexagonal phase, HP tridymite (Kihara 1978). In this phase the Si-O-Si angles from X-ray diffraction are all 180° if uncorrected for disorder (Kihara et al. 1986b). Because $M_1$ in HP tridymite at 420 °C is the same as in the LHP phase ($323 < T < 420$ °C) (Fig. 2a), the mean bond angles $\langle\alpha\rangle$ in LHP and HP tridymite are the same, 153.1°.

## Acknowledgments

We acknowledge NERC for research grant GR3/7496A. We thank R.J. Kirkpatrick for helpful discussions and for providing us with data prior to publication. We also thank R. Lamb, M. Lockyer, and D. Holland for help and advice on heat-flux DSC.

## References cited

Ashworth, J.R. (1989) Transmission electron microscopy of coexisting low-tridymite polymorphs. Mineralogical Magazine, 53, 89–97.

Baur, W.H. (1977) Silicon-oxygen bond lengths, bridging angles Si-O-Si and synthetic low tridymite. Acta Crystallographica, B33, 2615–2619.

Blinc, R. (1981) Magnetic resonance and relaxation in structurally incommensurate systems. Physics Reports, 79, 331–398.

Cellai, D., Carpenter, M.A., Wruck, B., and Salje, E.K.H. (1994) Characterization of high-temperature phase transitions in single crystals of Steinbach tridymite. American Mineralogist, 79, 606–614.

Cellai, D., Carpenter, M.A., Kirkpatrick, R.J., Salje, E.K.H., and Zhang, M. (1995) Thermally induced phase transitions in tridymite: An infrared spectroscopy study. Physics and Chemistry of Minerals, 22, 50–60.

De Dombal, R.F., and Carpenter, M.A. (1993) High temperature phase transitions in Steinbach tridymite. European Journal of Mineralogy, 5, 607–622.

Dollase, W.A. (1967) The crystal structure at 220 °C of orthorhombic high tridymite from the Steinbach meteorite. Acta Crystallographica, 23, 617–623.

Dollase, W.A., and Baur, W.H. (1976) The superstructure of meteoritic low tridymite solved by computer simulation. American Mineralogist, 61, 971–978.

Dupree, R., Kohn, S.C., Henderson, C.M.B., and Bell, A.M.T. (1993) The role of NMR shifts in structural studies of glasses, ceramics and minerals. In J.A. Tossell, Ed., Nuclear magnetic shieldings and molecular structure, vol. 386, p. 421–434. NATO ASI, Kluwer Academic, Dordrecht, the Netherlands.

Engelhardt, G., and Radeglia, R. (1984) A semi-empirical quantum-chemical rationalization of the correlation between Si-O-Si angles and $^{29}$Si NMR chemical-shifts of silica polymorphs and framework aluminosilicates (zeolites). Chemical Physics Letters, 108, 271–274.

Fyfe, C.A., Feng, Y., and Grondey, H. (1993) Evaluation of chemical shift-structure correlations from a combination of X-ray diffraction and 2D MAS NMR data for highly siliceous zeolite frameworks. Microporous Solids, 1, 393–400.

Graetsch, H., and Flörke, O.W. (1991) X-ray powder diffraction patterns and phase relationship of tridymite modifications. Zeitschrift für Kristallographie, 195, 31–48.

Hoffmann, W., Kockmeyer, M., Löns, J., and Vach, C. (1983) The transformation of monoclinic low tridymite MC to a phase with an incommensurate superstructure. Fortschritte der Mineralogie, 61, 96–98.

Kihara, K. (1977) An orthorhombic superstructure of tridymite existing between 105 °C and 180 °C. Zeitschrift für Kristallographie, 146, 185–203.

——— (1978) Thermal change in unit-cell dimensions and a hexagonal structure of tridymite. Zeitschrift für Kristallographie, 148, 237–253.

——— (1995) Disorder and successive structural transitions in the tridymite forms of $SiO_2$. Physics and Chemistry of Minerals, 22, 223–232.

Kihara, K., Matsumoto, T., and Imamura, M. (1986a) High temperature thermal-motion tensor analyses of tridymite. Zeitschrift für Kristallographie, 177, 39–52.

——— (1986b) Structural changes of orthorhombic-I tridymite with temperature: A study based on second-order thermal-vibration parameters. Zeitschrift für Kristallographie, 177, 27–38.

Löns, J., and Hoffmann, W. (1987) Zur kristallstructur der inkommensurablen raumtemperaturphase des tridymits. Zeitschrift für Kristallographie, 178, 141–143.

Nukui, A., Nakazawa, H., and Akao, M. (1978) Thermal changes in monoclinic tridymite. American Mineralogist, 63, 1252–1259.

Nukui, A., Yamamoto, A., and Nakazawa, H. (1979) American Institute of Physics Conference Proceedings, 33, p. 327.

Pettifer, R.F., Dupree, R., Farnan, I., and Sternberg, U. (1988) NMR determination of Si-O-Si bond angle distributions in silica. Journal of Non-crystalline Solids, 106, 408–412.

Phillips, B.L., Kirkpatrick, R.J., and Thompson, J.G. (1991) $^{29}$Si magic-angle spinning NMR spectroscopy of the ferroelastic-to-incommensurate transition in $Sr_2SiO_4$. Physical Review B, 43, 13280–13284.

Phillips, B.L., and Kirkpatrick, R.J. (1995) High temperature $^{29}$Si MAS NMR spectroscopy of anorthite ($CaAl_2Si_2O_8$) and its $P\bar{1} \rightarrow I\bar{1}$ structural phase transition. Physics and Chemistry of Minerals, 27, 268–276.

Smith, J.V., and Blackwell, C.S. (1983) Nuclear magnetic resonance of silica polymorphs. Nature, 303, 223–225.

Thompson, A.B., and Wennemer, M. (1979) Heat capacities and inversions in tridymite, cristobalite, and tridymite-cristobalite mixed phases. American Mineralogist, 64, 1018–1026.

Wennemer, M., and Thompson, A.B. (1984) Tridymite polymorphs and polytypes. Schweizerische Mineralogische und Petrographische Mitteilungen, 64, 335–353.

Withers, R.L., Thompson, J.G., Xiao, Y., and Kirkpatrick, R.J. (1994) An electron diffraction study of the polymorphs of $SiO_2$-tridymite. Physics and Chemistry of Minerals, 21, 421–433.

Xiao, Y., Kirkpatrick, R.J., and Kim, Y.J. (1993) Structural phase transitions of tridymite: A $^{29}$Si MAS NMR investigation. American Mineralogist, 78, 241–244.

——— (1995) Investigations of MX-1 tridymite by $^{29}$Si MAS NMR: Modulated structures and structural phase transitions. Physics and Chemistry of Minerals, 22, 30–40.

Manuscript received July 17, 1995
Manuscript accepted January 10, 1996